ELSEVIER

Polymer 44 (2003) 473–479

polymer

www.elsevier.com/locate/polymer

Crystallization of poly(ethylene terephthalate) under tensile strain: crystalline development versus mechanical behaviour

F. Chaari[a], M. Chaouche[a,*], J. Doucet[b]

[a]*Laboratoire de Mécanique et Technologie, Ecole Normale Supérieure de Cachan, Universite Paris 6, 61, Avenue du Président Wilson, 94235 Cachan Cedex, France*

[b]*Laboratoire d'Utilisation du Rayonnement Electromagnetique Bât 209D Centre Universitaire-B.P. 34-91898 Orsay Cedex, France*

Abstract

The crystallization of poly(ethylene terephthalate) (PET) under tensile strain was investigated using wide angle X-ray diffraction. Real-time investigation of the crystallization state, including the crystalline ratio and the crystallite orientation, of the material could be undertaken due to the high brilliance of the synchrotron X-ray source used in our study. Initially amorphous PET specimens were stretched at different strain rates and draw ratios at the same temperature (above and close to T_g). Our experimental set-up was designed to undertake simultaneous recording of the X-ray diffraction patterns and the mechanical parameters. Up to the draw ratio of 500% and draw rate of 0.75 s^{-1}, the crystalline development dynamics corresponded to three different regimes. (i) For small enough extension rates, there was no measurable crystallinity during the drawing process. The crystallization developed after cessation of deformation. (ii) For intermediate extension rates, the whole crystallization process took place during the deformation. (iii) For the highest extension rate involved in our experiments, the crystallization started during the drawing process and continued after cessation of deformation. The mechanical behaviour of the polymer was simultaneously recorded and correlated with the induced crystalline microstructure. In particular, we were able to discriminate the influence of crystallite orientation and crystallization growth on the mechanical behaviour of the material.

Keywords: Crystallization; Mechanical behaviour; X-ray diffraction

1. Introduction

Poly(ethylene terephthalate) (PET) is extensively used in industry in a semi-crystalline state to manufacture bottles, films, fibres, etc. The mechanical properties of the product are primarily a function of the crystalline texture, the crystalline volume fraction and the molecular orientation and extension. In addition to the thermal history, these parameters are strongly affected by the deformation/flow experienced by the polymer during its processing. Therefore, understanding the relationship between the deformation characteristics (strain rate, stress, geometry, etc.) and the induced microstructure (crystalline state, chain orientation and stretch) is vital in order to undertake quantitative predictions relative to the final properties (mechanical, optical, gas permeability, etc.) of the product.

In most of the studies reported in the literature [1–4] concerning the strain-induced crystallization of PET, the crystalline microstructure was analysed ex situ, after the completion of the deformation. In these experiments, the samples are subjected to different strain rates and draw ratios and quenched to room temperature at the end of the deformation process before analysing the crystalline microstructure. Such experimental procedure would not be able to address some of many questions raised in the literature concerning the effects of the deformation on the crystallization, including the role of molecular and crystallite relaxation, the relationship between mechanical behaviour and the induced microstructure, etc. The availability of high brilliance X-ray beams stemming from synchrotron radiation sources makes it possible now to undertake in situ experiments and therefore address the previous issues. Recently, Mahendrasingam et al. [5,8,9] and Blundell et al. [7] reported a series of experiments in which PET films were drawn slightly above T_g, and simultaneously, the X-ray diffraction patterns at rates as high as a pattern per 40 ms were recorded. They considered in particular the effect of the draw ratio, the temperature and the draw rate on the final crystallinity, the crystallization rate, and the level of molecular orientation that induces the start-up of a significant crystallization. Moreover, they reported the

* Corresponding author.
E-mail address: chaouche@lmt.ens-cachan.fr (M. Chaouche).

0032-3861/03/$ - see front matter © 2002 Published by Elsevier Science Ltd.
PII: S0032-3861(02)00739-5

intriguing phenomenon that above a certain draw rate (related to the relaxation time of the polymer), the deformation inhibited the crystallization growth process, and the later was delayed until the end of the deformation. However, it is not clear whether this is actually due to the inhibition of the crystallization process by the deformation or simply due to the fact that the final draw ratios are finite. Moreover, in the above in situ studies, the mechanical behaviour was not simultaneously recorded and correlated with the microstructure evolution. Finally, there is a need to undertake more synchrotron experiments in order to get deeper understanding of polymer crystallization under strain.

The purpose of the study reported here is twofold. We first follow the evolution of the crystallinity ratio along with the crystallite orientation during the specimen stretching, at different extension rates and draw ratios, and several minutes after cessation of mechanical deformation. The second purpose of this study is to correlate, at least qualitatively, the mechanical behaviour of the polymer with the crystalline development.

2. Experiments

The experiments were carried out at the Beamline D43 of the Laboratoire d'Utilisation du Rayonnement Electromagnetique (LURE) in Orsay (France). The wave length was 1.45 Å and the beam diameter 0.5 mm. The detector was a CCD X-ray camera placed at a distance of 65 mm from the sample, which insured the wide angle X-ray diffraction (WAXD) conditions. Sequences of video images were recorded using a video-tape recorder and later digitised and analysed using appropriate softwares. The integration time (time interval between two successive diffraction frames) was about 0.9 s. Real-time investigation could be undertaken at deformation rates as high as $0.75\ s^{-1}$. However, the deformation rates considered here remained below the ones for which Mahendrasingam et al. [5] reported a delayed appearance of the strain-induced crystallization until the end of the deformation. Thus, this phenomenon was not encountered in our study.

PET (PET 99 21 W EASTMAN) cone-shaped (in order to localize the deformation in its central region) specimens were prepared by injection moulding. Using the WAXD technique, we checked that the crystallization induced by this processing was negligible. Moreover, WAXD patterns were recorded during heating process (about 2 mn) to insure that there was no crystallization due to purely thermal effects. The specimens were 100 mm in length and 4 mm in thickness. They were drawn using a ZWICK tensile machine at a controlled velocity. A hot air blowing apparatus was used to heat the sample. The temperature could be adjusted by varying the air flow rate. In the present study, the temperature was set to 95 ± 2 °C, as measured using a thermocouple placed near the region through which the X-ray beam passed (initial mid-point of the specimen). The size of the heated region was about 25 mm. Using three thermocouples placed at different positions, we checked that the temperature was fairly uniform in the heated zone. However, due the thermal gradient between the latter and the part of the specimen that was outside the heating cell, the strain field was not homogeneous. Then, the draw rate in the zone where the microstructure was investigated using WAXD could not be inferred from the cross head speed. Necking phenomenon would also complicate this task. Therefore, measurement of local strain rate was required in order to link the actual draw rate to the corresponding induced microstructure. Unfortunately, an experimental set-up including such measurements turned out to be cumbersome while performing synchrotron experiments. Then, local strain measurements have been undertaken separately under the same thermo-mechanical conditions (temperature and cross head speeds). In order to determine the local strain field, a black painting was sprayed on the specimen's surface, and the time evolution of the spray pattern could be followed using a CCD camera associated with an image analyses software (OPTIMAS). The time evolution of the strain, and then the strain rate, were determined using a home-developed cross correlation technique. This technique is described in detail in Ref. [6], for instance. The strain rates were determined at the same position than that investigated in the WAXD experiments. The values reported below are averages over five different tensile tests performed under the same thermo-mechanical conditions.

3. Results and discussion

3.1. Evolution of the WAXD patterns during the deformation

In Fig. 1, we represent the evolution of the tensile stress against the draw ratio for the smallest initial extension rate ($0.06\ s^{-1}$) involved in our experiments. In order to determine the stress, we need to know the thickness of the specimen. The latter is estimated assuming that the material is incompressible, i.e. the Poisson ratio is equal to 0.5. The thickness as determined using this method is found to be consistent with the values estimated using the variation of the X-ray diffracted intensity during the drawing process.

We also represent in Fig. 1, a selected set of X-ray diffraction patterns corresponding to different positions on the stress–strain curve. The frame (f) represents the WAXD pattern obtained several minutes after cessation of the deformation, while the temperature is hold constant. Up to the draw ratio of 500% we do not observe any significant crystallization of the material. The intensity increase of the signal may be attributed to the decreasing of the specimen's thickness. Although there is no significant crystallization, we do observe a strain-hardening in the stress–strain curve. This result is consistent with the commonly accepted idea that the appearance of the strain-hardening can be attributed

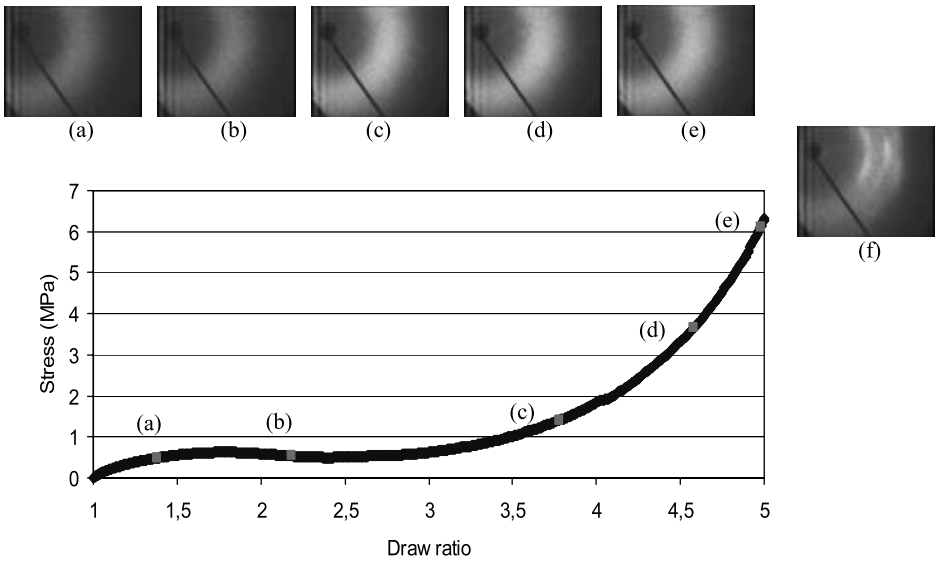

Fig. 1. Tensile stress as a function of overall draw ratio for a local extension rate of 0.06 s^{-1}. Above the graph, X-ray diffraction patterns are represented, corresponding to different labelled positions on the stress–strain curve. The frame (g) is obtained several minutes after cessation of the deformation.

the chain extension in a rubber-like material, where the crystal nuclei act as physical cross links. The crystallization growth develops essentially after the deformation. This is discussed in more detail in Section 3.2.

Fig. 2 is similar to Fig. 1, but in the case of a higher initial extension rate (0.2 s^{-1}). The frame (g) corresponds to the diffraction pattern obtained several minutes after cessation of the deformation, while the temperature was hold constant. There is no significant difference between frame (f) and frame (g). That is, under these experimental conditions (extension rate, draw ratio and temperature) the whole crystallization process takes place during the deformation, and there is no subsequent crystallization after cessation of extension. This is confirmed quantitatively below by determining the evolution of the crystalline ratio during the extension.

In Fig. 3, we represent the stress as a function of draw ratio along with a set of X-ray diffraction patterns corresponding to different positions on the stress–strain curve, in the case of a higher initial extension rate (0.75 s^{-1}). The results are qualitatively different from the case of a relatively small extension rate (Figs. 1 and 2). The frame (e), which corresponds to the end of the deformation is clearly different from the frame (f) which represents the X-ray pattern several minutes after cessation of deformation. For this higher extension rate, the crystallization

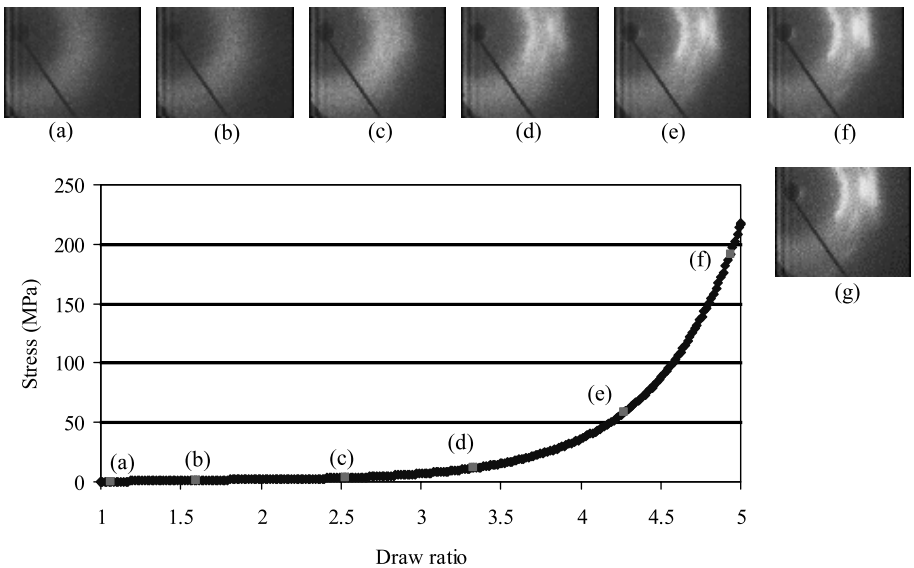

Fig. 2. Tensile stress as a function of draw ratio for an extension rate of 0.2 s^{-1}. A sequence of X-ray patterns are represented above the graph. Each frame corresponds to a given indicated position on the stress–strain curve. The frame (f) represents a WAXD pattern obtained several minutes after cessation of deformation.

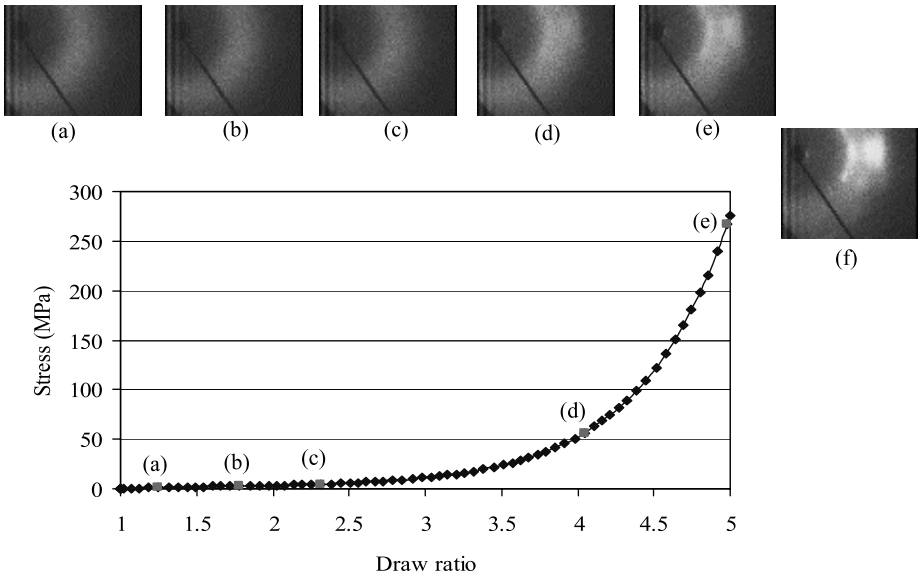

Fig. 3. stress as a function of draw ratio for an extension rate of 0.75 s^{-1}. A sequence of X-ray patterns are represented above the graph. Each frame corresponds to a given indicated position on the force–strain curve. The frame (f) represents a WAXD pattern obtained several minutes after cessation of deformation.

process starts during the extension and continues during the quiescent state. Moreover, the crystallinity is quite low at the end of deformation, it is clearly smaller than the one obtained at the end of the deformation at a smaller extension rate (Fig. 2). This is discussed more quantitatively farther.

3.2. Evolution of the crystallite orientation and crystallinity ratio versus mechanical stress

The crystalline unit cell of PET is known to be triclinic and its parameters has been determined by Daubeny et al. [10]. The crystallite orientation of PET in terms of the angle between the *c*-axis of the unit cell and the drawing direction can be characterized by the normal to the lattice plane $(\bar{1}05)$ [11,12]. However, the corresponding reflection occurs at quite large scattering angle (43°), and could not be detected using our experimental set-up. Moreover, even detected the intensity of this reflex is known to be rather small. To determine the crystallite orientation, Wilchinsky [11] showed that instead of the $(\bar{1}05)$ reflection, one can use the three equatorial reflections (010), $(\bar{1}10)$ and (100). He showed that the angle σ, that these planes make with the *c*-axis fulfils the following relationship [14]:

$$\langle\cos^2\sigma\rangle = 1 - 0.87\langle\cos^2\sigma_{(010)}\rangle - 0.77\langle\cos^2\sigma_{(\bar{1}10)}\rangle - 0.34\langle\cos^2\sigma_{(100)}\rangle$$

where

$$\langle\cos^2\sigma_{(hkl)}\rangle = \frac{\int_0^{\pi/2} I_{(hkl)}(\phi)\sin\phi\cos^2\phi\,\mathrm{d}\phi}{\int_0^{\pi/2} I_{(hkl)}(\phi)\sin\phi\,\mathrm{d}\phi}$$

In this expression $I_{(hkl)}$ is the intensity of the reflection (*hkl*), ϕ is the azimuthal angle and (*hkl*) = (010), $(\bar{1}10)$ or (100).

It is more convenient to discuss the crystallite orientation in terms of the Herman's orientation function:

$$fc = \frac{3\langle\cos^2\sigma\rangle - 1}{2}$$

$fc = 1$ when the chains are perfectly oriented along the draw direction, and $fc = 0$ when they are randomly oriented. The reflections (010), $(\bar{1}10)$ and (100) are azimuthally scanned and the Herman orientation function is calculated using the intensity profiles. This is illustrated in Fig. 4.

In order to estimate the crystallinity, the diffraction patterns are scanned along the radial direction for both the amorphous (taking into account the thickness variation) and the semi-crystalline states. The crystalline ratio is then estimated to be the ratio of the area of the intensity profile under the peaks (corrected for the amorphous contribution) to the total area. The calculation method is illustrated in Fig. 5, and this is described in detail in Ref. [13]. The main origin of uncertainty in the determination of the crystallinity from WAXD patterns is related to the separation of the amorphous halo from the total intensity. Actually, it is known that this method is less accurate than that based on density measurements for instance. However, it is not clear how to use the latter in our in-situ experiments.

The orientation function and the crystallinity ratio for different extension rates are represented as a function of draw ratio in Fig. 6a. The development of the strain-induced crystalline microstructure is compared to the evolution of the mechanical stress (Fig. 6b). We quantitatively confirm here the qualitative trends reported above.

Fig. 6 shows that the crystallite orientation function remains almost constant during the crystallization growth. This is an indication that the orientation of the crystallites is already pre-determined during, and even before, the nucleation process. It is to be noted that before a significant

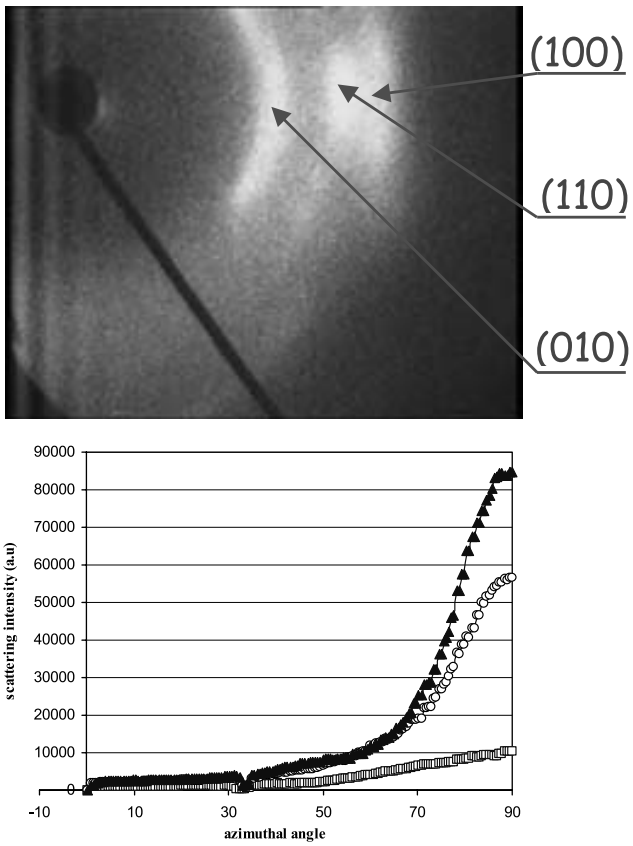

Fig. 4. Illustration of the method used to extract an azimuthal intensity profile to calculate the Herman orientation function. (▲): (100); (□): (010); (○): ($\bar{1}$10).

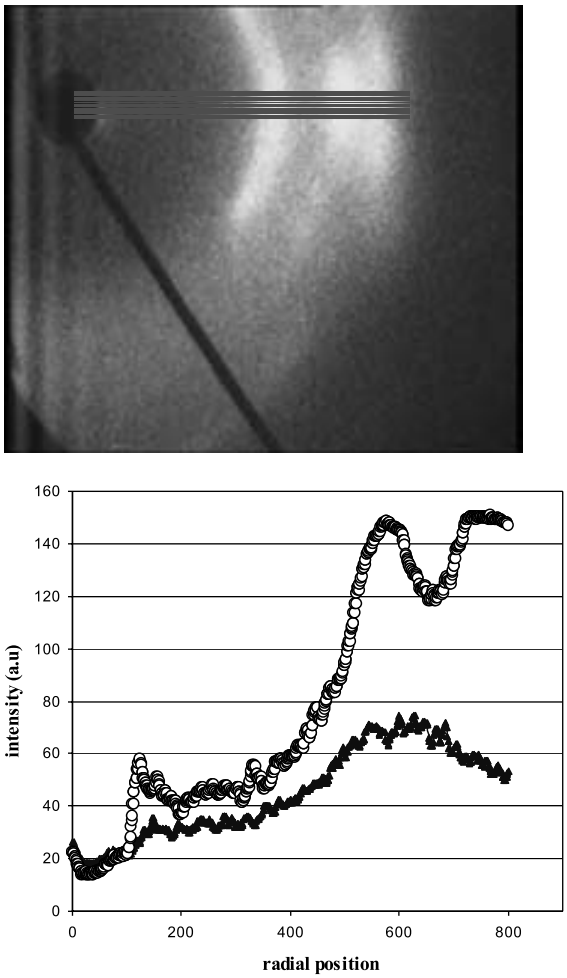

Fig. 5. Illustration of the method used to extract a radial intensity profile in order to estimate the crystallinity ratio. The integration region is indicated on the WAXD pattern. (▲): amorphous; (□): crystalline.

crystallization growth, the crystalline orientation function cannot be determined accurately from the WAXD patterns. It would be more appropriate to use other techniques such as infrared spectroscopy [15]. The final chain orientation seems to be independent upon the extension rate, at least for the values considered here. Moreover, there is no detectable relaxation of the crystallite orientation after cessation of the deformation. This may be understood by the fact that when the polymer is in a semi-crystalline state its effective viscosity is so high that the chain relaxation time is much larger than the extension characteristic times involved in our experiments. In order to estimate the relaxation time of the crystallites, one needs to know the crystallite size. This can be inferred from the diffraction pattern using the Scherrer relationship:

$$L_{(hkl)} = \frac{\lambda}{\cos\,\theta_{(hkl)} \times \Delta\theta_{(hkl)}}$$

where $L_{(hkl)}$ is the crystallite size in the (hkl) direction, λ, the X-ray wave length ($\lambda = 1.45$ Å), $\theta_{(hkl)}$ the scattering angle and $\Delta\theta_{(hkl)}$ the width at half high of the intensity profile along the radial direction. The crystallite sizes can be evaluated using the reflections ($\bar{1}$05) whose plane normal is close to the chain axis), (100) whose plane normal is close to the benzene ring and (010) [11]. As it is indicated above, the first reflection cannot be detected using our experimental set-up. Then, only the crystallite size along the directions perpendicular to the chains can be estimated. The intensity profiles are fitted using a Pearson II function [16] and the crystallite size along (100) and (010) can be estimated. For all the WAXD patterns analysed, these two sizes are found almost equal and independent on the draw ratio. The estimated value is about (30λ). Our crystallite size measurements are consistent to those reported by Vigny et al. [1], in the case of similar but ex-situ experiments.

The crystallite size in the drawing direction for PET cannot be measured here, but we can use the results of Vigny et al. [1] to infer an order of magnitude. Contrary to the crystallite sizes in the direction perpendicular to the *c*-axis, Vigny et al. [1] found that the size along this axis (length) was highly sensitive to the thermo-mechanical conditions (temperature, draw ratio) and the molecular weight. However, the crystallite length was always higher than the lateral sizes and its value was found to be on the order of 40λ.

Let us then assume that the crystallites are approximately

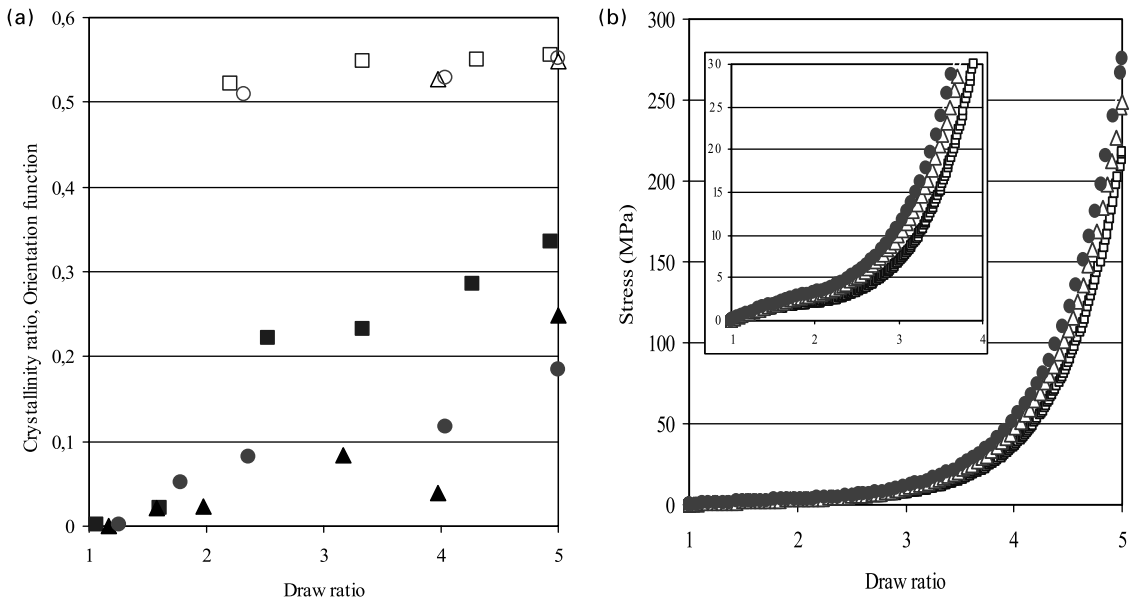

Fig. 6. Evolution of crystallite orientation function and the crystalline ratio as a function of draw ratio (Fig. 6a). This figure correlates the crystalline development with the mechanical behaviour (Fig. 6b). For Fig. 6a (▲, △): 0.55 s^{-1}; (●, ○): 0.75 s^{-1}; (■, □): 0.2 s^{-1}. For Fig. 6b (△): 0.55 s^{-1}; (●): 0.75 s^{-1}; (○): 0.2 s^{-1}.

spherical solid objects immersed in a viscous matrix (amorphous phase). The characteristic orientational relaxation time (due to Brownian motion) of these objects can be estimated as [17]:

$$\tau = \frac{\pi \mu L^3}{6 K_B T}$$

where μ is the viscosity of the matrix, L the crystallite size (we take $L = 40\lambda$), K_B the Boltzmann constant ($K_B = 1.38 \times 10^{-23}$J/K) and T the temperature ($T = 368$ K). The viscosity may be estimated from the measured stress using the relationship: $\sigma \sim \mu\dot{\gamma}$. The minimum rotary relaxation time that can be estimated from our experimental results (minimum viscosity for which the crystallinity is detectible) is then: $\tau \approx 4000\,\text{s} > 1\,\text{h}$. This is much larger than the characteristic time of the deformation rates involved in our experiments ($1/\dot{\epsilon}_0$, where $\dot{\epsilon}_0$ is the strain rate). This may explain then why the orientation function of the crystallites is independent on the draw ratio. At the end of the deformation the effective viscosity of the material is higher and the crystallite length is also higher, which may dramatically increase the rotary relaxation time of the crystallites. Indeed, we do not observe any significant change in the crystallite orientation even several minutes after the cessation of the deformation.

Fig. 6 shows that significant crystallization growth starts approximately at the point where the material becomes strain-hardening. The value of the crystalline ratio after cessation of the deformation is not represented in this figure for clarity. As expected the crystallization growth is faster at high draw rates, however, the value of the crystalline ratio at the end of the crystallization process is almost independent on the draw rate.

The connection between the mechanical behaviour of the material and the crystalline development has already been discussed in the literature [1,4]. However, this discussion was based on ex-situ experiments. In such experiments, there is the question about the influence of the quenching process on the crystalline microstructure. Nevertheless, our on-line measurements are consistent with the previously reported ideas. This may be summarized as follows. At small draw ratios there is no measurable crystallinity and the material has a linear visco-elastic behaviour (linear portion of the stress–strain curve). In this region, the polymer would be in an uncross-linked amorphous state. This is followed by some kind of a plateau during which oriented nuclei would develop. The last part of the stress–strain curve (strain-hardening) corresponds to the crystallization growth.

4. Concluding remarks

Real-time investigation has been undertaken into the crystallization under tensile strain of PET in order to correlate the crystalline texture development with the material mechanical behaviour. Up to the strain rate of 0.75 s^{-1} and draw ratio of 500%, the crystallization development followed three different regimes. At quite small extension rates, there was no measurable (using our WAXD set-up) crystallinity development during the deformation. There was, however, a significant effect of the deformation on the subsequent crystallization, which developed after cessation of the deformation under isothermal and constant strain conditions. For intermediate strain rates, the whole crystallization process was found to

take place during the deformation. At higher extension rates, the crystallization process was found to start during the deformation and continued after cessation of the extension under isothermal and constant strain conditions. We can anticipate that if one increases further the draw rate, the crystallization may start after cessation of the deformation as it has been observed by Mahendrasingam et al. [5].

Our on-line measurements confirm the generally reported ideas concerning the relationship between the microstructure development and the mechanical behaviour of the material. Thus, the stress–strain curve can be divided into three regions corresponding to different material microstructure states. There is a visco-elastic region in which the polymer chains are subjected to thermal relaxation and strain orientation and extension in an amorphous matrix. We could not consider the microstructure evolution in this region since the X-ray diffraction technique is more appropriate for analysing rather crystalline structures. This first region would be followed by a nucleation region in which oriented nuclei would act as physical cross links. Finally, our study clearly shows that the strain-hardening of the material coincides with the start-up of the crystallization growth.

Acknowledgements

We are indebted to W. Aussell and L. Chevalier for their help in the experiments.

References

[1] Vigny M, Tassin JF, Giraud A, Lorentz G. Polym Engng Sci 1997; 37(11):1785.
[2] Salem DR. Polymer 1992;33:3182.
[3] Le Bourvellec G, Monnerie L. Polymer 1986;27:856.
[4] Gorlier E, Haudin JM, Billon N. Polymer 2001;42:9541.
[5] Mahendrasingam A, Martin C, Fuller W, Blundell DJ, MacKerron DH, Oldman J, Harvie JL, MacKerron DH, Riekel RC, Engström P. Polymer 1999;40:5553.
[6] Chevalier L, Calloch S, Hild F, Marco Y. Eur J Mech A/Solids 2001; 20:169.
[7] Blundell DJ, Mahendrasingam A, Martin C, Fuller W, MacKerron DH, Harvie JL, Oldman RJ, Riekel C. Polymer 2000;41:7793.
[8] Mahendrasingam A, Martin C, Fuller W, Blundell DJ, Oldman RJ, MacKerron DH, Harvie JL, Riekel RC. Polymer 2000;41:1217.
[9] Mahendrasingam A, Blundell DJ, Martin C, Fuller W, MacKerron DH, Harvie JL, Oldman RJ, Riekel RC. Polymer 2000;41:7803.
[10] Daubeny RP, Bunn CW, Brown CJ. Proc R Soc London 1954;A(226): 531.
[11] Wilchinsky ZW. J Appl Phys 1959;30:792.
[12] Wilchinsky ZW, Advances in X-ray Analysis, vol. 6. New York: Plenum Press; 1963.
[13] Vainstein BK. Diffraction of X-rays by chain molecules. Amsterdam: Elsevier; 1966.
[14] Göshel U, Deutscher K, Abetz V. Polymer 1996;37:1.
[15] Matthews RG, Ajji A, Dumoulin MM, Prud'homme RE. Polymer 2000;41:7139.
[16] Hall MM, Veeraraghavan VG, Rubin H, Winchell PG. J Appl Crystallogr 1977;10:66.
[17] Doi M, Edwards SF. J Chem Soc Faraday Trans II 1975;74:1789.